

Crossing the Gap from p - to n -Type Doping: Nature of the States near the Chemical Potential in $\text{La}_{2-x}\text{Sr}_x\text{CuO}_4$ and $\text{Nd}_{2-x}\text{Ce}_x\text{CuO}_{4-\delta}$

P. G. Steeneken,¹ L. H. Tjeng,^{1,2} G. A. Sawatzky,^{1,3} A. Tanaka,⁴ O. Tjernberg,^{5,6} G. Ghiringhelli,^{6,7} N. B. Brookes,⁶ A. A. Nugroho,¹ and A. A. Menovsky⁸

¹*MSC, University of Groningen, Nijenborgh 4, 9747 AG Groningen, The Netherlands*

²*II. Physikalisches Institut, Universität zu Köln, Zùlpicher Straße 77, 50937 Köln, Germany*

³*Department of Physics, University of British Columbia, Vancouver, Canada BC V6T 1Z4*

⁴*Department of Quantum Matter, ADSM Hiroshima University, Higashi-Hiroshima 739-8526, Japan*

⁵*LMSP, Royal Institute of Technology, Electrum 229, S-164 40 Kista, Sweden*

⁶*European Synchrotron Radiation Facility (ESRF), BP 220, F-38043 Grenoble, France*

⁷*INFN, Dipartimento di Fisica, Politecnico di Milano, 20133 Milano, Italy*

⁸*Van der Waals-Zeeman Laboratory, University of Amsterdam, 1018 XE Amsterdam, The Netherlands*
(Received 2 February 2003; published 19 June 2003)

We report on an x-ray absorption and resonant photoemission study on single crystals of the high- T_c cuprates $\text{La}_{2-x}\text{Sr}_x\text{CuO}_4$ and $\text{Nd}_{2-x}\text{Ce}_x\text{CuO}_{4-\delta}$. Using an intrinsic energy reference, we find that the chemical potential of $\text{La}_{2-x}\text{Sr}_x\text{CuO}_4$ lies near the top of the La_2CuO_4 valence band whereas in $\text{Nd}_{2-x}\text{Ce}_x\text{CuO}_{4-\delta}$ it is situated near the bottom of the Nd_2CuO_4 conduction band. The data clearly establish that the introduction of Ce in Nd_2CuO_4 results in electrons being doped into the CuO_2 planes. We infer that the states closest to the chemical potential have a Cu $3d^{10}$ singlet origin in $\text{Nd}_{2-x}\text{Ce}_x\text{CuO}_{4-\delta}$ and a $3d^9\bar{L}$ singlet origin in $\text{La}_{2-x}\text{Sr}_x\text{CuO}_4$.

DOI: 10.1103/PhysRevLett.90.247005

PACS numbers: 74.25.Jb, 71.18.+y, 74.72.-h, 79.60.-i

One of the long-standing puzzles in the field of high- T_c superconductivity concerns the nature of the charge carriers in doped high- T_c cuprates [1]. Several photoemission studies [2–4] have revealed very little difference between the valence band spectra of the $\text{Nd}_{2-x}\text{Ce}_x\text{CuO}_{4-\delta}$ and $\text{La}_{2-x}\text{Sr}_x\text{CuO}_4$ systems. In particular, the position of the chemical potential in the two different systems seems to be quite similar and is located in the gap of the parent compounds, while one would expect that the chemical potential should shift from the top of the valence band to the bottom of the conduction band by changing from p -type to n -type doping. From this unexpected behavior it was concluded that both hole and electron doping result in new states that fill the band gap. Several explanations have been proposed for this midgap pinning of the chemical potential [2,5–7], with perhaps the scenario involving the occurrence of phase separation to be currently the most discussed [5,7,8]. In addition, for $\text{Nd}_{2-x}\text{Ce}_x\text{CuO}_{4-\delta}$ it has even become an issue whether it can be regarded as a really electron doped system [9–11], since transport measurements have revealed a positive Hall coefficient [12,13]. This has led to propositions that the charge carriers relevant for the superconductivity in $\text{Nd}_{2-x}\text{Ce}_x\text{CuO}_{4-\delta}$ are holelike.

In this paper we present a comparative x-ray absorption (XAS) and resonant photoemission (RESPES) study on $\text{Nd}_{2-x}\text{Ce}_x\text{CuO}_{4-\delta}$ and $\text{La}_{2-x}\text{Sr}_x\text{CuO}_4$ single crystals. To ensure that the spectra collected are representative for the bulk material, we rely on the bulk sensitivity of the x-ray absorption technique as well as of valence band photoemission measurements using high photon energies [14]. In addition, we use an intrinsic energy reference within

the CuO_2 planes as proposed earlier [5], in order to ensure a reliable measurement of the position of the chemical potential relative to the valence band. We find unambiguously that the chemical potential μ of $\text{La}_{2-x}\text{Sr}_x\text{CuO}_4$ lies near the top of the La_2CuO_4 valence band and μ of $\text{Nd}_{2-x}\text{Ce}_x\text{CuO}_{4-\delta}$ lies near the bottom of the Nd_2CuO_4 conduction band, and that the introduction of Ce results in electrons being doped into the CuO_2 planes. Resonance data suggest that the charge carriers in $\text{Nd}_{2-x}\text{Ce}_x\text{CuO}_{4-\delta}$ are different in nature than in $\text{La}_{2-x}\text{Sr}_x\text{CuO}_4$, in the sense that they are singlets of Cu $3d^{10}$ character rather than of $3d^9\bar{L}$, where \bar{L} denotes an oxygen ligand hole [15]. In addition we find that the presence of Nd $4f$ states and a different O $2p$ to Cu $3d$ charge transfer energy cause $\text{Nd}_{2-x}\text{Ce}_x\text{CuO}_{4-\delta}$ to have an *apparently* similar chemical potential position as $\text{La}_{2-x}\text{Sr}_x\text{CuO}_4$ if the leading edge of the main valence band structure is used as reference.

Single crystals of Nd_2CuO_4 , $\text{Nd}_{1.85}\text{Ce}_{0.15}\text{CuO}_{4-\delta}$, La_2CuO_4 , and $\text{La}_{1.85}\text{Sr}_{0.15}\text{CuO}_4$ were grown by the traveling solvent floating zone method [16]. From ac-susceptibility measurements the onset of the superconducting transition in the $\text{La}_{1.85}\text{Sr}_{0.15}\text{CuO}_4$ sample is $T_c = 35$ K. The $\text{Nd}_{1.85}\text{Ce}_{0.15}\text{CuO}_{4-\delta}$ crystals show a critical temperature of 21 K after reducing them in flowing N_2 gas at 900 °C for 30 h. XAS and RESPES experiments were performed at the ID12B beam line of the ESRF. The overall energy resolution was set to 0.3 eV for the XAS and 0.5 eV for the RESPES. The samples were both cleaved and measured at 20 K in a chamber with a base pressure below 5×10^{-11} mbar. Core level x-ray photoemission (XPS) was carried out in Groningen.

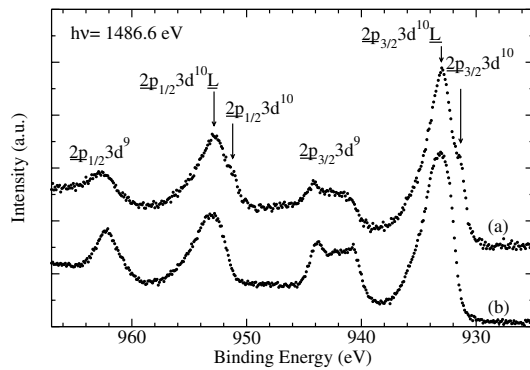


FIG. 1. Room temperature Cu $2p$ XPS spectra of (a) $\text{Nd}_{1.85}\text{Ce}_{0.15}\text{CuO}_{4-\delta}$ and (b) Nd_2CuO_4 .

Figure 1 shows the Cu $2p$ core level XPS of Nd_2CuO_4 and $\text{Nd}_{1.85}\text{Ce}_{0.15}\text{CuO}_{4-\delta}$ where we have used the standard labeling for the structures [4,17]. We clearly observe that the $2p3d^9$ “satellites” decrease in intensity with Ce doping, and that also new structures, labeled as $2p3d^{10}$, start to appear on the low binding energy side of the $2p3d^{10}\underline{L}$ “main lines,” with $2p$ denoting a $2p$ core hole. These spectra imply that Ce doping results in a decrease of the Cu^{2+} content with the $3d^9$ and $3d^{10}\underline{L}$ configurations, and simultaneously in an increase of the Cu^{1+} with the $3d^{10}$ configuration. In other words, electrons are indeed introduced into the CuO_2 planes.

Figure 2 depicts the Cu L_3 XAS spectrum of Nd_2CuO_4 and $\text{Nd}_{1.85}\text{Ce}_{0.15}\text{CuO}_{4-\delta}$ normalized to the Nd M_5 absorption line as shown in the inset. The Cu white line is given by the transition $3d^9 + h\nu \rightarrow 2p3d^{10}$. One can clearly see that the Cu white line intensity has decreased appreciably when Ce is introduced into the system, consistent with the results from earlier electron energy loss studies on polycrystalline samples [18]. This directly indicates again that the Cu^{2+} content in the CuO_2 plane is reduced, i.e., Ce doping indeed means electron doping.

Having established that $\text{Nd}_{2-x}\text{Ce}_x\text{CuO}_{4-\delta}$ is an electron doped material, we now shift our focus to the issue of the position of the chemical potential in $\text{Nd}_{2-x}\text{Ce}_x\text{CuO}_{4-\delta}$ relative to that in $\text{La}_{2-x}\text{Sr}_x\text{CuO}_4$ and

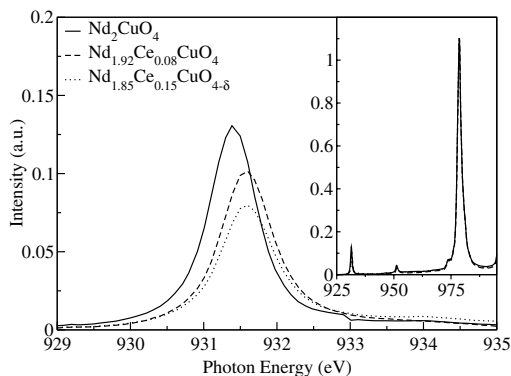


FIG. 2. Cu L_3 XAS spectra of $\text{Nd}_{2-x}\text{Ce}_x\text{CuO}_{4-\delta}$ normalized on the Nd M_5 absorption intensity as shown in the inset.

their parent materials. Figure 3 shows the on- and off-resonance photoemission spectra of $\text{Nd}_{1.85}\text{Ce}_{0.15}\text{CuO}_{4-\delta}$, Nd_2CuO_4 , La_2CuO_4 , and $\text{La}_{1.85}\text{Sr}_{0.15}\text{CuO}_4$. The on-resonance spectra are taken with the photon energy tuned at the maximum of the Cu L_3 XAS white line, and the off-resonance spectra with a photon energy which is 5.0 ± 0.1 eV lower. It has been demonstrated earlier [19,20] that the Cu L_3 resonant photoemission spectrum of Cu^{2+} oxides is dominated by the autoionization process of the type $3d^9 + h\nu \rightarrow 2p3d^{10} \rightarrow 3d^8$, thereby enhancing the spectral weight of the $3d^8$ final states considerably. Indeed, the spectra depicted in the top panel contain the characteristic 1G and 3F structures of a $3d^8$.

We now will use the $3d^8$ 1G peak to set the energy scale for all the photoemission spectra [5], since this will give us an energy zero that refers directly to the electronic structure of the CuO_2 plane, which is at the heart of the current discussion. Such an intrinsic energy reference is much more reliable than using the leading edge of the main peak of the off-resonance valence band spectrum [2,3], since in comparing the $\text{Nd}_{2-x}\text{Ce}_x\text{CuO}_{4-\delta}$ with the $\text{La}_{2-x}\text{Sr}_x\text{CuO}_4$ system one can suffer from differences due to the presence of different chemical species and charge transfer energies, as we will show later. It is also better to use the intrinsic energy reference rather than the Fermi level of the spectrometer [6], since the chemical potential of the undoped Nd_2CuO_4 and La_2CuO_4 is not

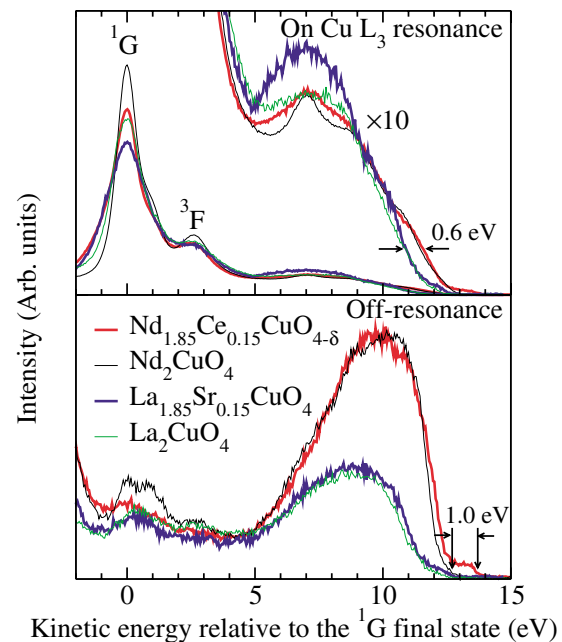


FIG. 3 (color). Upper panel: resonant photoemission of $\text{Nd}_{1.85}\text{Ce}_{0.15}\text{CuO}_{4-\delta}$, Nd_2CuO_4 , La_2CuO_4 , and $\text{La}_{1.85}\text{Sr}_{0.15}\text{CuO}_4$ at the Cu L_3 edge. The energies of the spectra are aligned on the Cu $3d^8$ 1G final states. Lower panel: off-resonance spectra at a photon energy 5 eV below the resonance. Arrows indicate the valence band onset of Nd_2CuO_4 and the Fermi level of $\text{Nd}_{1.85}\text{Ce}_{0.15}\text{CuO}_{4-\delta}$.

well defined and in fact can even be pinned by impurities or defects of unknown nature and quantities.

With the 1G peak position set to zero, we can clearly observe in the lower panel of Fig. 3 that the first ionization state of $\text{Nd}_{1.85}\text{Ce}_{0.15}\text{CuO}_{4-\delta}$ is about 1.0 eV further away than that of the undoped Nd_2CuO_4 . Recalling that the onset of the optical gap in Nd_2CuO_4 is approximately 1.0 eV (with the first peak in the optical spectrum at 1.5 eV) [21,22], one can immediately conclude that the chemical potential of the Ce doped system lies near the bottom of the conduction band of the undoped Nd_2CuO_4 . We thus conclude that the chemical potential for the doped material is not pinned in the middle of the gap of the undoped material. A similar conclusion has also been reached recently from doping dependent angle-resolved photoemission experiments [23], although there one needs to assume that one can align the spectrum of the undoped Nd_2CuO_4 with respect to that of the $\text{Nd}_{2-x}\text{Ce}_x\text{CuO}_{4-\delta}$ by using the leading edge of the valence band for small doping levels.

In comparing $\text{La}_{2-x}\text{Sr}_x\text{CuO}_4$ with La_2CuO_4 using the 1G intrinsic reference, we can also clearly see from the lower panel of Fig. 3 that the chemical potential in $\text{La}_{1.85}\text{Sr}_{0.15}\text{CuO}_4$ resides in the vicinity of the top of the valence band of La_2CuO_4 , contrary to earlier reports in which the chemical potential was concluded to be pinned in the middle of the insulator gap [3,6]. We suspect that this discrepancy is caused by the different method for the energy referencing, which can lead to hidden energy shifts, as we have explained above. Our finding connects well with very recent studies indicating that in hole doped oxychloride cuprates the chemical potential is also near the top of the valence band [24,25].

The lower panel of Fig. 3 also shows that the valence band spectrum of Nd_2CuO_4 is very different in intensity and also in energy position as compared to the spectrum of La_2CuO_4 . We can identify two reasons for this. The first is that in the $\text{Nd}_{2-x}\text{Ce}_x\text{CuO}_{4-\delta}$ system the presence of Nd contributes significantly to the valence band spectrum, while this is not the case for La in $\text{La}_{2-x}\text{Sr}_x\text{CuO}_4$. From photoionization cross-section tables [26], one can estimate that the Nd $4f$ is responsible for more than 50% of the signal in $\text{Nd}_{2-x}\text{Ce}_x\text{CuO}_{4-\delta}$ at the photon energies used, while in $\text{La}_{2-x}\text{Sr}_x\text{CuO}_4$ the spectrum is dominated by the Cu spectral weight. It is also important to realize that the Nd $4f$ signal is present over the entire valence band energy range. This is demonstrated by Fig. 4, where we plot the resonant photoemission spectrum of the Nd_2CuO_4 and $\text{Nd}_{1.85}\text{Ce}_{0.15}\text{CuO}_{4-\delta}$ valence bands, with the photon energy tuned on the Nd $3d$ absorption edge. From these data we could even infer that the top of the valence band in the undoped Nd_2CuO_4 consists of Nd $4f$ states and not of Cu $3d^9\bar{L}$. Perhaps this is why it is difficult to dope holes into the CuO_2 planes in T' cuprates, as they would go into the Nd-O planes.

Another cause for differences in the valence band spectrum of Nd_2CuO_4 as compared to La_2CuO_4 is laid out in

the upper panel of Fig. 3. A blowup of the Cu L_3 on-resonance photoemission spectra shows that the leading edge of the valence band in Nd_2CuO_4 and also $\text{Nd}_{1.85}\text{Ce}_{0.15}\text{CuO}_{4-\delta}$ is higher in energy by about 0.6 eV than in La_2CuO_4 . This agrees very well with the fact that the optical gap in Nd_2CuO_4 is about 0.5 eV smaller than in La_2CuO_4 (which has its first peak in the optical spectrum at 2.0 eV) [21,22]. One could infer that this 0.6 eV difference reflects the difference in the effective O $2p$ -Cu $3d$ charge transfer energy, since this parameter determines the magnitude of the band gap of the insulating correlated cuprates. On hindsight, it is perhaps not surprising to find such differences in view of the fact that Nd_2CuO_4 and La_2CuO_4 have different crystal structures and O-Cu bond lengths, resulting in differences in Madelung potentials and O $2p$ -Cu $3d$ hopping integrals. In fact, there is no compelling reason to believe that a comparative study of the development of the chemical potential in $\text{Nd}_{2-x}\text{Ce}_x\text{CuO}_{4-\delta}$ can be carried out using $\text{La}_{2-x}\text{Sr}_x\text{CuO}_4$ as a reference.

Finally, we study the character of the states closest to the Fermi level (E_F) in the electron doped system. Figure 5 shows the on- and off-resonance photoemission spectrum of $\text{Nd}_{1.85}\text{Ce}_{0.15}\text{CuO}_{4-\delta}$ in the vicinity of the top of the valence band and the near E_F region. As expected, the on-resonance intensity is enhanced as compared to the off-resonance one. However, the enhancement is substantially smaller than that for the hole doped cuprates, as one can clearly see from Fig. 5, which also includes the on- and off-resonance data for $\text{La}_{1.85}\text{Sr}_{0.15}\text{CuO}_4$ and $\text{Bi}_2\text{Sr}_2\text{CaCu}_2\text{O}_8$. Since at the L_3 resonance the Cu $3d^8$ spectral weight is being measured, the enhancements for the near E_F states basically indicate the amount of $3d^8$ character that is mixed into these states. For the undoped cuprates, cluster calculations have shown that the states near the top of the valence band consist of Zhang-Rice singlets having mainly a $3d^9\bar{L}$ character, and also about

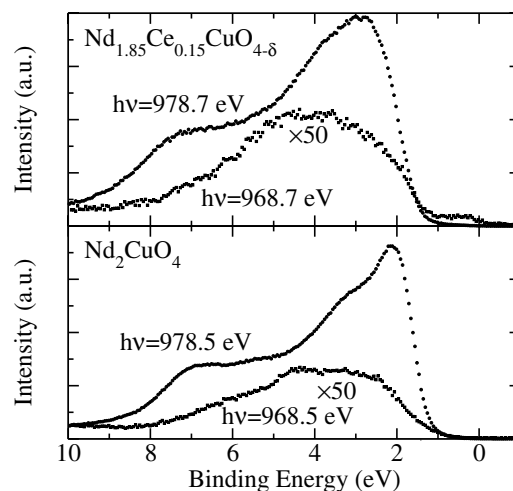


FIG. 4. On- and off-resonance photoemission spectra at the Nd M_5 absorption edge.

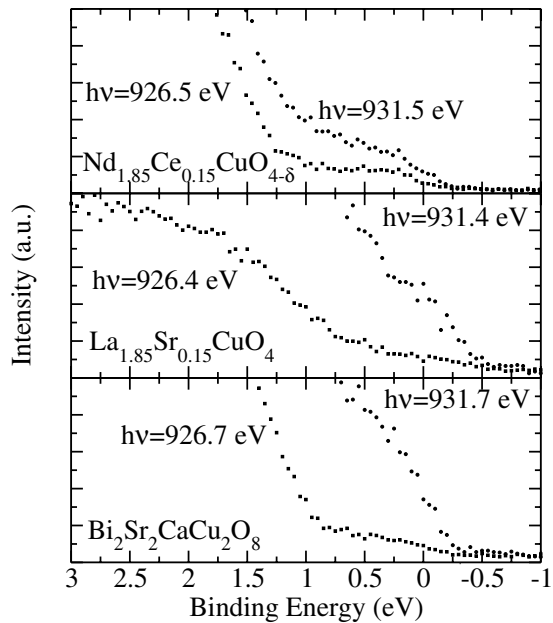


FIG. 5. On- and off-resonance photoemission spectra at the Cu L_3 absorption edge.

8% $3d^8$ admixture due to the direct hybridization between these two local configurations [27,28]. RESPE studies, including also hole doped cuprates, have confirmed this picture [19,29]. The much smaller resonance enhancement factor for the near E_F intensity in $\text{Nd}_{1.85}\text{Ce}_{0.15}\text{CuO}_{4-\delta}$ implies a much smaller admixture of the $3d^8$ states, indicating that these near E_F states do not have a direct hybridization with the $3d^8$. We conclude that these states are not of local $3d^9\bar{L}$ character, and we infer that they are in fact $3d^9$ final states that are reached by the photoemission process starting from a $3d^{10}$ initial state. In this framework, the $3d^9$ state has to hybridize with a neighboring $3d^9\bar{L}$ cluster, to acquire the $3d^8$ character reached in the resonance process. These data thus support the scenario that the charge carriers in $\text{Nd}_{2-x}\text{Ce}_x\text{CuO}_{4-\delta}$ are electrons of singlet $3d^{10}$ nature.

To conclude, we have measured that the CuO_2 planes in the $\text{Nd}_{2-x}\text{Ce}_x\text{CuO}_{4-\delta}$ high- T_c cuprates are electron doped. Using a reliable intrinsic energy reference we have established that the chemical potential in $\text{La}_{2-x}\text{Sr}_x\text{CuO}_4$ and $\text{Nd}_{2-x}\text{Ce}_x\text{CuO}_{4-\delta}$ is not pinned in the middle of the gap of the insulating parent compounds. Instead, it is located in the vicinity of the top of the valence band for $\text{La}_{2-x}\text{Sr}_x\text{CuO}_4$, and near the bottom of the conduction band for $\text{Nd}_{2-x}\text{Ce}_x\text{CuO}_{4-\delta}$. One might say that it crosses the gap upon going from p - to n -type doping. It is important to note that the existence of phase separation [5–8] in the doped materials could involve the pinning of the chemical potential inside the gap, but that our results indicate that this pinning could not take the chemical potential very far away from the band

edges, with perhaps a value of 0.3 eV as an upper limit judging from our experimental resolution and uncertainties in determining the onset of the optical gap. Resonance data suggest that the charge carriers in $\text{Nd}_{2-x}\text{Ce}_x\text{CuO}_{4-\delta}$ are electrons of Cu $3d^{10}$ character, while in $\text{La}_{2-x}\text{Sr}_x\text{CuO}_4$ and $\text{Bi}_2\text{Sr}_2\text{CaCu}_2\text{O}_8$ they are $3d^9\bar{L}$ -like holes. As far as symmetry is concerned, the charge carriers in both the electron and hole doped cuprates are singlet in nature.

We thank K. Larsson and A. Heeres for their skillful technical assistance and N. P. Armitage, J. W. Allen, and A. Fujimori for valuable discussions. This work was supported by the Netherlands Foundation for Fundamental Research on Matter (FOM), the Netherlands organization for Scientific Research (NWO), and by the Deutsche Forschungsgemeinschaft through SFB 608, as well as by KNAW 95-BTM-33.

- [1] M. Imada *et al.*, Rev. Mod. Phys. **70**, 1039 (1998).
- [2] J. W. Allen *et al.*, Phys. Rev. Lett. **64**, 595 (1990).
- [3] H. Namatame *et al.*, Phys. Rev. B **41**, 7205 (1990).
- [4] T. Suzuki *et al.*, Phys. Rev. B **42**, 4263 (1990).
- [5] R. O. Anderson *et al.*, Phys. Rev. Lett. **70**, 3163 (1993).
- [6] N. Harima *et al.*, Phys. Rev. B **64**, 220507(R) (2001).
- [7] A. Damascelli *et al.*, J. Electron Spectrosc. Relat. Phenom. **117–118**, 165 (2001).
- [8] V. J. Emery and S. A. Kivelson, J. Phys. Chem. Solids **53**, 1499 (1992).
- [9] L. Jansen and R. Block, Physica (Amsterdam) **271A**, 169 (1999).
- [10] H. A. Blackstead and J. D. Dow, Solid State Commun. **107**, 323 (1998).
- [11] J. E. Hirsch and F. Marsiglio, Physica (Amsterdam) **162C–164C**, 591 (1989).
- [12] Z. Z. Wang *et al.*, Phys. Rev. B **43**, 3020 (1991).
- [13] W. Jiang *et al.*, Phys. Rev. Lett. **73**, 1291 (1994).
- [14] A. Sekiyama *et al.*, Nature (London) **403**, 396 (2000).
- [15] Z.-X. Shen and D. S. Dessau, Phys. Rep. **253**, 1 (1995).
- [16] A. A. Nugroho *et al.*, Phys. Rev. B **60**, 15379 (1999).
- [17] H. Ishii *et al.*, Jpn. J. Appl. Phys. **28**, L1952 (1989).
- [18] M. Alexander *et al.*, Phys. Rev. B **43**, 333 (1991).
- [19] L. H. Tjeng *et al.*, Phys. Rev. Lett. **67**, 501 (1991).
- [20] N. B. Brookes *et al.*, Phys. Rev. Lett. **87**, 237003 (2001).
- [21] S. Uchida *et al.*, Physica (Amsterdam) **162C–164C**, 1677 (1989).
- [22] S. Uchida *et al.*, Phys. Rev. B **43**, 7942 (1991).
- [23] N. P. Armitage *et al.*, Phys. Rev. Lett. **88**, 257001 (2002).
- [24] Y. Kohsaka *et al.*, cond-mat/0209339.
- [25] F. Ronning *et al.*, Phys. Rev. B **67**, 165101 (2003).
- [26] J. J. Yeh and I. Lindau, At. Data Nucl. Data Tables **32**, 1 (1985).
- [27] F. C. Zhang and T. M. Rice, Phys. Rev. B **37**, 3759 (1988).
- [28] H. Eskes *et al.*, Phys. Rev. B **41**, 288 (1990).
- [29] L. H. Tjeng *et al.*, Phys. Rev. Lett. **78**, 1126 (1997).